2008

Cytotoxicity of Diepoxybutane and Epichlorohydrin in Relation to Stages of the Cell Cycle

Megan L. Watts
Colby College

Cytotoxicity of Diepoxybutane and Epichlorohydrin in Relation to Stages of the Cell Cycle

Megan L. Watts

A Thesis Presented to the Department of Biology,
Colby College, Waterville, ME
In Partial Fulfillment of the Requirements for Graduation
With Honors in Biology

Submitted May 2008

Cytotoxicity of Diepoxybutane and Epichlorohydrin in Relation to Stages of the Cell Cycle

Megan L. Watts

Approved:

Julie T. Millard

(Mentor: Dr. Julie T. Millard, Professor of Chemistry)

May 21, 2008 Date

Paul G. Greenwood

(Reader: Dr. Paul G. Greenwood, Professor of Biology)

5-21-2008 Date

Lynn G. Hannum

(Reader: Dr. Lynn G. Hannum, Assistant Professor of Biology)

5/23/08 Date

Vitae

Megan Lindsay Watts was raised in Tenants Harbor, Maine, a small coastal town on the St. George Peninsula. She is the eldest of the three daughters of Lauren B. Watts, an occupational therapist, and H. Todd Watts, a merchant marine engineer, and a sister to Alexandra M. Watts and Taylor A. B. Watts. She was taught at St. George Elementary School and attended Georges Valley High School in Thomaston, Maine. She excelled academically in many subjects, but developed a genuine passion for the biological sciences under the tutelage of Mr. Kevin Vencile. The unexpected death of a childhood friend and classmate with brain cancer prompted her to explore a career in medicine.

In the fall of 2004, Megan began her undergraduate education at Colby College, where she pursued a major in biology as a premedical student. She conducted biochemistry research with Dr. Julie T. Millard during her junior and senior years, and completed two internships in the Millard Lab during the summers of 2007 and 2008. In addition to her academic pursuits, Megan enjoyed volunteering in a kindergarten classroom and the day surgery department at MaineGeneral Medical Center: Thayer Unit. Highlights of her time at Colby include pitching for the varsity softball team during her freshmen year and shadowing local OB/GYN and Colby alumna, Dr. Karen Bossie ('96).

In May 2008, Megan was awarded the Samuel R. Feldman Prize for excellence in premedical studies by Colby College. She will attend medical school in the fall with interests in pediatrics, obstetrics and gynecology, and hematology/oncology. Megan graduated with a Bachelor of Arts with honors in Biology and a minor in Chemistry.

Acknowledgments

I would like to express my gratitude to Dr. Julie T. Millard for her expertise, guidance, and patience in the completion of this honors project. Working as a research assistant in her lab was the most academically rewarding experience during my time at Colby. Dr. Millard was a great mentor, instilling by example the virtue of hard work, the importance of thoroughness, and the necessity of critical thinking. Her leadership and enthusiasm for biochemical research made this project possible.

Special thanks are owed to my readers, Dr. Paul G. Greenwood and Dr. Lynn G. Hannum, for taking time out of their busy schedules to help with this project. Thank you, Dr. Greenwood, for relaying your cell culture expertise and supporting me in my goal of becoming a physician. Thank you, Dr. Hannum, for guiding me through flow cytometry and for being a great advisor and an even better listener.

Thank you to Adam Newman ('07) for passing on his wealth of knowledge through many helpful conversations and always making lab work entertaining. Thank you to Erin McGowan ('08) and Matt Stein ('08) for being supportive lab partners.

Additionally, I would like to thank my friends and loved ones for their continued support, understanding, and encouragement. Thank you for your flexibility during a senior year filled with challenging classes, an honors project, and medical school applications.

Perhaps most importantly, I would like to thank my parents, Todd and Lauren Watts, for their unconditional love, support, and confidence in my abilities. You have made all that I do possible. Thank you to my sisters, Aley and Taylor, for always making me smile.

Table of Contents

List of Figures and Tables

Abstract

Work conducted in the Millard Biochemistry Research Laboratory examines the dual nature of molecules as carcinogens and anti-tumor agents through the molecular mechanisms of duplex DNA damage by bifunctional alkylating agents. Diepoxybutane (DEB) and epichlorohydrin (ECH) are polar molecules that form covalent DNA interstrand lesions by cross-linking the N7 position of deoxyguanosine residues. A recent experiment indicated that ECH preferentially targets nuclear DNA over mitochondrial DNA, whereas DEB shows similar rates of lesion formation for both loci. It was concluded that preferential targeting of nuclear DNA results from relatively poor uptake of ECH across the mitochondrial membrane. The objective of my honors research was to determine if the cytotoxicities of DEB and ECH vary according to the presence of the nuclear envelope in 6C2 chicken erythro-progenitor cells. The cytotoxicity of DEB and ECH was compared between cells randomly distributed throughout the cell cycle (G_0/G_1 and S >> G_2/M) and cells enriched in G_2/M stages. Results indicated that ECH is more cytotoxic than DEB in both unsynchronized control 6C2 cells and synchronized 6C2 cells enriched in G_2/M stages of the cell cycle. Treatment with either bifunctional alkylating agent induced greater cytotoxicity in 6C2 cells enriched in G_2/M stages than in unsynchronized control 6C2 cells, suggesting that the presence of the nuclear envelope—or any plasma membrane—may inhibit the reactivity of DEB and ECH.

Introduction

It has been almost a decade since cancer surpassed heart disease as the leading cause of death for Americans 85 years of age and younger[1]. Though the annual mortality rates of both diseases have exhibited a downward trend, it is apparent that the treatment of cancer continues to challenge both the medical and scientific communities. In 2008, more than 565,650 cancer-related deaths are predicted to occur in the United States alone, a country where 1 in 2 men and 1 in 3 women will battle a variety of cancers in their lifetimes[2]. The probability of developing some form of malignancy during one's lifetime is influenced by various factors, such as exposure to carcinogens in the environment and our lifestyle choices. Likewise, an individual's genetic composition determines his or her predisposition toward developing cancer.

Studies conducted in the Millard Biochemistry Research Laboratory aim to elucidate the molecular mechanisms of duplex DNA damage by bifunctional alkylating agents to gain insight into the dual nature of molecules that can act as carcinogens or anti-tumor agents. Also known as cross-linkers, these molecules have been used as chemotherapeutic agents since the chance discovery of the lymphotoxic action of nitrogen mustards during World War I[3].

The cytotoxic mechanisms of the bifunctional alkylators diepoxybutane (DEB) and epichlorohydrin (ECH) are of particular interest (Figure 1). These small, relatively polar molecules contain two reactive moieties that form covalent DNA interstrand lesions by preferentially cross-linking the N7 position of deoxyguanosine residues on opposite strands[4,5,6]. Interstrand cross-links interfere with the normal cellular process of replication fork progression during DNA synthesis and may potentially disrupt transcription if not repaired. Nucleotide-excision repair, homologous recombination, alkyltransferases, and

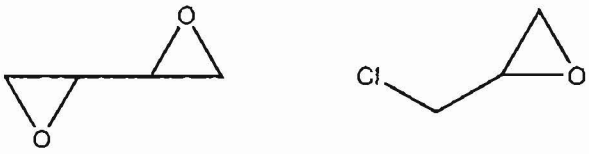

Diepoxybutane **Epichlorohydrin**

Figure 1. Chemical structures of diepoxybutane and epichlorohydrin. The structure of DEB contains two epoxide rings. ECH is characterized by two functionalities: an expoxide ring and a terminal chloride.

the Fanconi Anemia repair pathway are known to correct interstrand lesions resulting from reaction with bifunctional alkylating agents[7].

DEB is a metabolite of 1,3-butadiene (BD), a chemical used in the synthetic elastomer industry. BD is most abundantly used during the polymerization of styrene-butadiene rubber[6,8,9]. In addition to industrial chemistry, BD is an environmental air pollutant produced by internal combustion engines and cigarette smoke[8]. Prior to the 1980s, occupational exposure to BD was relatively unregulated with a Permissible Exposure Limit (PEL) of 1,000 ppm set by OSHA. However, studies performed in the 1980s on BD exposure in rat models indicated that the agent metabolizes to active compounds with definitive carcinogenic properties. This prompted OSHA to lower its ceiling PEL from 1,000 ppm to 10 ppm[10,11].

Genotoxic effects of DEB include DNA interstrand cross-links in mouse hepatocytes, sister chromatid exchange (SCE) or recombination, and chromosomal aberrations in cultured cell models. Employees exposed to BD and its physiological metabolite DEB exhibit statistically significant increases in the development of hematopoietic cancers[12,13,14]. The World Health Organization's International Agency for Research on Cancer (IARC) currently classifies DEB as a probable human carcinogen. Animal models provide sufficient evidence for carcinogenicity, but data linking human cancer cases directly to DEB exposure without other confounding variables are limited[15].

Additionally, DEB is commonly used to test for the Fanconi Anemia (FA) cellular phenotype. Patients with hereditary FA have mutations in proteins of the FA DNA repair

pathway, which promotes the repair of stalled replication forks during DNA synthesis. Impairment of FA repair mechanisms leads to cellular hypersensitivity to DNA interstrand cross-links, resulting in prolongation and ultimate arrest within the G_2 stage of the cell cycle[7,16,17,18].

DEB, a four-carbon molecule containing two symmetric epoxide rings, reacts predominantly with the N7 position of deoxyguanine residues during the formation of interstrand cross-links[4,5]. The nitrogen at position 7 of the guanine ring is the most nucleophilic atom in DNA. In addition to high electrophilicity, the location of N7 makes it sterically available for reaction with larger molecules (Figure 2). N7 first opens one epoxide ring through nucleophilic attack at the secondary, less-substituted carbon. The process is repeated by a guanine N7 residue on the opposing strand of duplex DNA, which opens the second epoxide ring and forms the covalent linkage. Negatively charged oxygens resulting from the loss of the two epoxide rings are protonated under physiological conditions (Figure 2)[6,9]. DEB preferentially targets 5' GNC sequences, where N is representative of either guanine or cytosine residues[4,19].

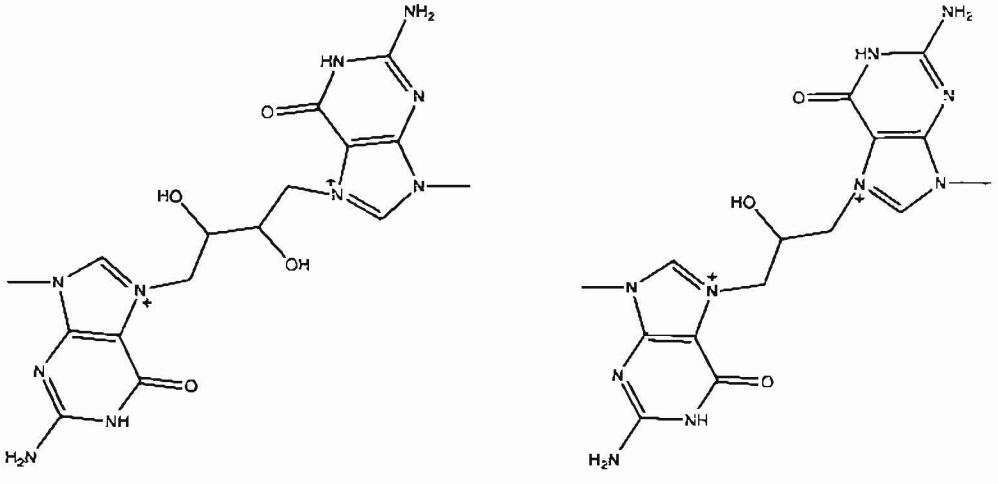

Figure 2. Chemical structures of covalent DNA interstrand cross-links. LEFT: DEB forms a cross-link between deoxyguanosine residues on opposing strands of DNA[6,9]. RIGHT: ECH cross-links two deoxyguanosine residues of duplex DNA[21]. The positive charge on the N7 nitrogen makes these cross-links very unstable; it has been proposed that such instability leads to the breakdown of the DNA double helix.

Epichlorohydrin is commonly used as an intermediate in the synthesis of products such as epoxy resins, synthetic glycerine, and surfactants in the polymer industry[20]. Research performed with yeast and mice systems by Van Duuren and Goldschmidt suggests that epoxide-containing compounds are largely mutagenic and likely have carcinogenic properties arising from their ability to modify DNA[6,21].

Approximately 80,000 US employees were occupationally exposed to ECH between 1981-1983[20]. OSHA designates the PEL for ECH at 2 ppm TWA (time-weighed average reflecting an 8-hour work shift)[10,11]. Human exposure to 20 ppm ECH leads to irritation of mucosal membranes, nausea, dyspnea, and englargement of the liver. Brief exposure to ECH concentrations about 100 ppm results in lung edema and kidney lesions[10,11]. Experiments that examine incidence of exposure to ECH and cancer rates among employees suggest a significantly higher risk of developing lung cancer, although the link between ECH and malignancy is controversial[20,22]. Currently, the IARC classifies both ECH and DEB as probable human carcinogens[15].

ECH has the potential for nucleophilic attack by the N7 deoxyguanine residue at both the less-substituted epoxide ring carbon and the carbon-chlorine bond (Figure 2). ECH targets both 5' GNC and 5' GC sequences, where N is representative of either guanine or cytosine residues[23]. During the formation of a mono-adduct through reaction with ECH, N7 acts as a nucleophile and opens the epoxide ring by attack at the secondary carbon. The negatively charged oxygen atom performs an S_N2 reaction, releasing chloride and forming a new epoxide ring. The N7 of a guanine residue located on the complementary strand nucleophilically attacks the new ECH epoxide ring at the less substituted carbon, creating a covalent interstrand cross-link. Under aqueous conditions, the negatively charged oxygen is protonated[22,23].

We are interested in the relationship between DEB and ECH toxicity and the relative availability of DNA throughout the cell cycle. Accumulation of DNA damage is a hallmark of

unregulated cell proliferation. Normally, the process is controlled by the cell cycle, a cyclic progression of four stages—G_1, S, G_2, and M—in which a cell prepares for its ultimate division (Figure 3). Cells not actively preparing to divide are said to be in the G_0 stage of the cell cycle, a period when the normal function of a specific cell type is performed. Binding of growth factor hormones, or mitogens, stimulates a cell to enter into the cell cycle at G_1 by initiating gene expression for regulatory cyclin-dependent kinase complexes (CdkC's). The relative concentrations of CdkC's drive the cell through each stage of the cell cycle, as many of the stage-specific complexes regulate the transcription and/or degradation of other regulatory enzymes[24,25].

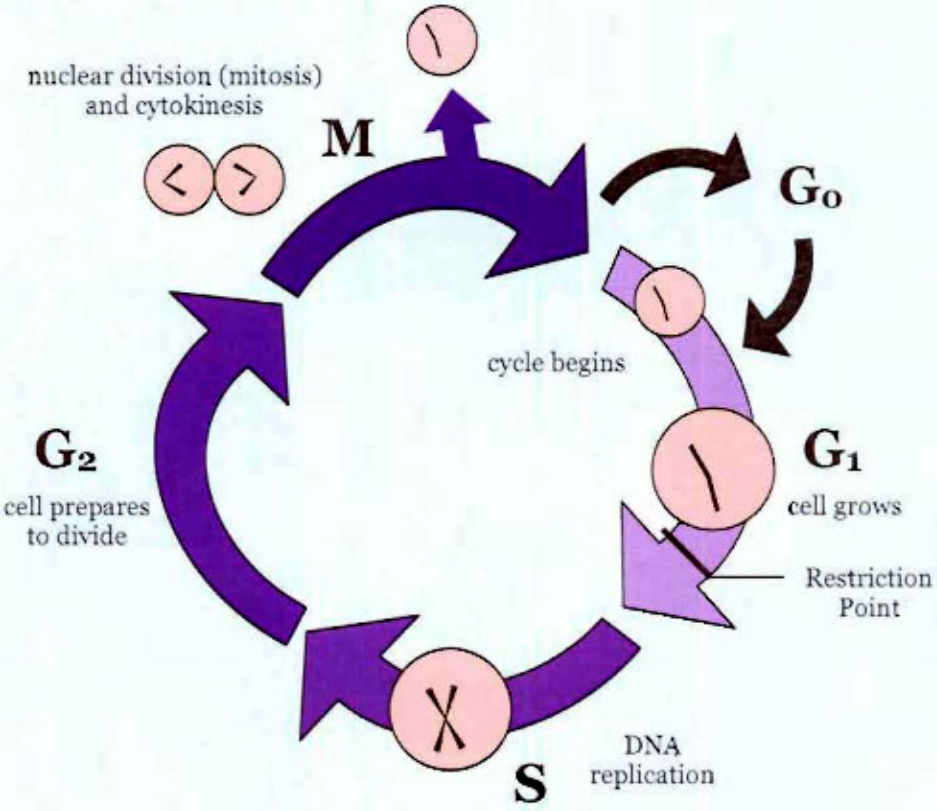

Figure 3. Schematic diagram of the cell cycle, illustrating the progression from G_1 through M. Cells may enter into the cell cycle from dormancy (G_0) or directly after cell division in highly proliferative populations.

Cells in G_1—"Gap 1"—undergo growth and perform damage control to monitor the results of the most recent cell division. Given enough stimulation via hormonal signaling for regulatory complexes, cells will pass the restriction point and enter into S stage: DNA synthesis. Progression past the restriction point commits the cell to division. G_2, also known as "Gap 2," is a time of cellular growth and damage control leading up to entry into M stage[24,26].

Mitosis consists of four phases: prophase, metaphase, anaphase, and telophase. The process of nuclear division begins with prophase, during which DNA condenses into chromosomes, the nuclear envelope disintegrates, and mitotic spindle fibers form and attach to chromosomes at kinetochores. Each of the above processes is facilitated by the maturation-promoting factor (MPF), the M stage Cdk1-Cyclin B1 complex. Notably, MPF phosphorylates nuclear lamins A, B, and C at serine residues, causing a conformational change to occur in scaffolding proteins and stimulating the depolymerization of the filaments that compose the lamin structure. Lamin B remains bound to nuclear membrane vesicles via a hydrophobic isoprenyl group at the C-terminus[24,27,28].

During metaphase, chromosomes align along the equatorial axis of the cell. Sister chromatids separate and move to each of the two poles through microtubule deploymerization at the kinetochore. The poles of the cell also increase the distance between one another in preparation for cytokinesis through molecular motor movement, polymerization of polar microtubules, and depolymerization of astral microtubles. Telophase marks the final step in nuclear division, during which the nuclear envelope reassembles, DNA decondenses, and mitotic spindles depolymerize. These steps are facilitated by the polyubiquination of Cyclin B1 and consequent degradation of MPF. Phosphorylation events performed by MPF during prophase are reversed via the dephosphorylation of cellular proteins by phosphatases[24,27].

Cytokinesis, or cellular division, is the final step of the M stage. Breakdown of MPF, which phosphorylates an inhibitory residue on myosin light chains within the cleavage furrow, allows for the activation of myosin. Contractile interactions between myosin and action result in complete cellular cleavage[24].

As illustrated by the various signaling pathways of the cell cycle, healthy cells are fully integrated with the extracellular environment and other neighboring cells, only entering the cell cycle when the summation of stimulatory signals is greater than that of inhibitory signals for cell division. As the degree of genomic instability increases, progeny of afflicted cells fail to respond to extracellular communication via growth factors and other hormone signals. These cells, having fallen out of synch with their environment, experience the disruption of signaling pathways that causes cells to display erratic behavior, namely uncontrolled cell division[29].

Under most conditions unfavorable genetic mutation results in cytotoxic effects and cell death; however, mutations affecting the activity of proto-oncogenes and tumor suppressor genes that are part of various DNA repair pathways may result in the deregulation of the cell cycle and give rise to cancer. One commonly affected pathway includes p53, a tumor suppressor gene, which mediates an important cell cycle checkpoint in the presence of DNA damage[27,30]. Arrest of the cell cycle allows for the repair of damage sustained during a previous phase. The absence or complete avoidance of cell cycle checkpoints compromises the genetic fitness of the cell; hence, signal molecules involved in checkpoints and cell cycle arrest are vital to normal function and proliferation[27,31]. As previously stated, cells displaying the FA phenotype arrest in G_2 when exposed to DEB[7,16,17,18]. Human diploid fibroblasts treated with ECH at doses above 0.5 mM/hour arrest in G_1 6-18 hours after initial exposure[32].

Additionally, mutations to kinases and phosphatases involved in signaling pathways may result in the overexpression of regulatory elements and have similar deleterious effects on the normal progression of the cell cycle. Interestingly, lymphomas, liver and lung tumors

resulting from DEB exposure in murine models are characterized by activated K-Ras oncogenes and lymphoma-specific p53 mutations[15].

The most recent study completed by the Millard Biochemistry Research Team examined the relationship between chromatin structure and DNA damage by DEB, ECH, and the related epihalohydrin, epibromohydrin (EBH), at three loci: expressed nuclear DNA, unexpressed nuclear DNA, and "naked" mitochondrial DNA. 6C2 chicken erythro-progenitor cells were treated independently with 250 mM of the three bifunctional alkylating agents for various incubation times. Quantitative polymerase chain reaction (QPCR) was performed using a limited amount of template DNA isolated from the treated cells. QPCR compares the amount of amplification of control, untreated DNA to that from cells treated with the agent in question[33]. QPCR data were analyzed via the Poisson expression; plots were constructed for lesion frequency versus incubation time, showing a linear trend-line with a slope equal to the lesion frequency per unit time[34].

Data indicated that nuclear DNA damage occurs at comparable levels for DEB, ECH, and EBH treated cells, regardless of chromatin structure ("open" expressed versus "condensed" unexpressed). The study also found that ECH and EBH preferentially target nuclear DNA over mitochondrial DNA, whereas DEB shows similar rates of lesion formation for both loci. A three to four-fold increase in lesion formation occurred for both nuclear heterochromatin and euchromatin treated with ECH or EBH versus treated mitochondrial DNA. The conclusion was that preferential targeting of nuclear DNA results from relatively poor uptake of ECH and EBH across the mitochondrial membrane[35]. In general, compounds experience poor mitochondrial uptake as a result of small, polar chemical composition; the high lipid-to-DNA ratio of mitochondria favor the uptake of larger, lipophilic molecules[36].

In this study, we sought to investigate the cytotoxicity of DEB and ECH in relation to the cell cycle. Specifically, the main objective of the study was to determine whether the presence of the nuclear envelope significantly influences the cytotoxicity of DEB and ECH.

6C2 chicken erythro-progenitor cells served as our model cell line; exposure to many bifunctional alkylating agents corresponds to an increase in the risk of developing various hematopoeitic cancers, making organelle-containing erythro-progenitor cells an optimal system for our topic of study[12,13,14].

The cytotoxicity of DEB and ECH was compared between populations of cells randomly distributed throughout the cell cycle (G_0/G_1 and S >> G_2/M) and those populations of cells enriched in G_2/M stages. LD_{50} values were determined for 30 minute, 60 minute, 120 minute, and 180 minute treatment periods for each of the four categories: DEB unsynchronized control cells, DEB cells enriched in G_2/M stages, ECH unsynchronized control cells, and ECH cells enriched in G_2/M stages. It is our hope that investigating the role of the cell cycle in relation to DEB and ECH will provide insight into the carcinogenic nature of these bifunctional alkylators.

Materials and Methods

Cell Culture. 6C2 chicken (*Gallus gallus*) erythro-progenitor cells were cultured in growth media composed of MEM Richter's modification with L-glutamine, 10% heat-inactivated fetal bovine serum, 2% heat-inactivated chicken serum, 1 mM HEPES buffer, 50 μM β-mercaptoethanol, 88 units/mL penicillin, 88 μg/mL streptomycin, and 0.2 μg/mL amphotericin B. Cells were grown in T25 culture flasks maintained at 37 °C and 5% CO_2. 85-90% confluent 6C2 cell suspensions were passaged by 1:5 (1 mL cell suspension and 4 mL culture media), 1:10 (1 mL cell suspension and 9 mL culture media), or 1:20 (0.5 mL cell suspension and 9.5 mL culture media) dilutions to maintain the cell line. Informal measurements by Newman (unpublished data) suggest a population doubling time of 6-8 hours and approximately 2 days of growth for 6C2 chicken erythro-progenitor cells to reach 85-90% confluence.

Additional 6C2 cells from the first three passages were frozen and stored in liquid nitrogen for preservation of the cell line. The contents of one T-25 culture flask were transferred to a 15 mL conical Falcon tube and centrifuged at 300 x *g* for 5 minutes. The supernatant was removed and discarded. The pellet was suspended in cold 6C2 cell culture media supplemented with 10% DMSO to achieve a concentration of 1×10^6 to 1×10^7 cells/mL. 1 mL aliquots of the cell suspension were transferred to individual Corning® cryovials and placed at -70 °C overnight. Vials were then moved to liquid nitrogen storage indefinitely.

The integrity of a cell line becomes drastically diminished after 20-25 passages as a result of numerous selection events that gradually alter the genetic composition of the cells. New cell lines were initiated from stocks in liquid nitrogen storage. A single vial was removed from liquid nitrogen and thawed rapidly by heat from the palms of hands. Taking care to prevent contamination of the cells, the cryovial was wiped with 70% ethanol before opening.

The contents of the vial were transferred to a 15 mL conical Falcon tube and 9 mL of fresh 6C2 culture media was introduced in a drop-wise manner with occasional mixing of the suspension. Cells were centrifuged at 250 x *g* for 5 minutes. The supernatant containing culture media supplemented 10% DMSO was removed and discarded. The pellet was suspended in 10 mL of fresh 6C2 culture media and transferred to a T-25 culture flask at 37 °C and 5% CO2.

Synchronization of Cells. Nocodazole, a chemical synchronizing agent, arrests cells in a prophase to "pseudo-metaphase" stage of mitosis[37]. The antimitotic agent inhibits microtubule polymerization by binding to beta-tubulin and disrupting the formation of interchain disulfide linkages[38]. Nocodazole also prevents the degradation of cyclin B1; cells cannot exit mitosis because the Cdk1-CyclinB1 complex (MPF) remains intact and active[39]. The low toxicity and reversible nature of nocodazole make the agent useful for obtaining enriched mitotic populations of cells for studies of the cell cycle.

10 mL of 6C2 cells at 85-90% confluence were transferred to a T-75 culture flask containing 20 mL of growth media supplemented with 30 μL of 0.4 mg/mL nocodazole (final concentration of 400 ng/uL nocodazole) and incubated at 37 °C and 5% CO_2 for 16 hours. The cell suspension was transferred to a 50 mL conical Falcon tube and centrifuged at 250 x g for 5 minutes. The supernatant containing the cellular synchronization agent was removed and discarded and the pellet was washed with 5 mL of fresh 6C2 culture media and centrifuged as above. Again, the supernatant was removed and discarded. Cells were suspended in 30 mL of fresh 6C2 culture media, transferred in 5 mL aliquots to a six-well plate, and incubated at 37 °C and 5% CO_2 for approximately 3-4 hours before treatment with DEB or ECH.

Cell Cycle Analysis. Flow cytometric analysis was performed on live 6C2 chicken erythro-progenitor cells to determine the relative distribution of cells in the G_0/G_1, S, and G_2/M stages of the cell cycle under normal growth conditions. In flow cytometry, a given population of cells is stained with one or more fluorescent, DNA-specific dyes. Stains used exclusively for cell cycle analysis are membrane-permeant and non-fluorescent until bound to DNA, allowing for the analysis of live populations of cells without prior fixation. Upon excitation of the dye, the level of fluorescence emitted by the labeled DNA of each individual cell is proportional to the DNA mass of the cell. Cells in the G_0/G_1 stage contain one set of paired chromosomes (2N), cells in S stage contain a variable amount of DNA between one and two sets of paired chromosomes as a result of current DNA replication, and cells within G_2/M stages contain two sets of paired chromosomes (4N)[40]. Hence, cells at the G_2/M stages of the cell cycle emit twice the level of fluorescence as cells in G_0/G_1 emit, and so on. Cell cycle analysis of 6C2 chicken erythro-progenitor cells used Invitrogen Vybrant® DyeCycle Green™ DNA stain, which is excited by the 488 nm wavelength laser line of a flow cytometer and emits fluorescence at approximately 520 nm[40].

Cell cycle analysis was performed before each assay involving synchronized 6C2 cells to verify successful enrichment of the population of cells arrested in G_2/M by treatment with nocodazole. 1 mL of the synchronized cell suspension was removed from the control well (6 mL total volume) of the six-well plate and transferred to a sterile flow cytometry tube. 1 mL of a control cell suspension at a concentration of approximately 1×10^6 cells/mL was transferred from a T-25 culture flask to another sterile flow cytometry tube. Cellometer™ automatic cell counting device determined the concentration of the cell suspension. Samples were prepared for flow cytometry by the addition of 2 µL of Vybrant® DyeCycle Green™ stain to each tube. Each sample was protected from light and incubated at 37 °C for 30 minutes[40].

Flow cytometry data was collected with BD Biosciences CellQuest™ software. FACSCalibur fluorescence detectors were set at 328 V (FL1), 605 V (FL2), and 350 V (FL3)

while the scattering detector was assigned 210 V (SSC). The mode of the FL1 detector was set to linear rather than logarithmic; this provided better definition of population peaks during analysis. A histogram of frequency versus fluorescence/emission was constructed from the flow cytometry data of 10,000 cellular events. Regions were applied to data in order to exclude dead cells and inert debris from analysis. Gates were drawn around the G_0/G_1 and G_2/M cell populations and corresponding histogram statistics were calculated for the percentages of total cells falling within each defined gate.

Treatment with DEB and ECH. Cytotoxicity studies were conducted for DEB with unsynchronized cells, ECH with unsynchronized cells, DEB with cells arrested in G_2/M, and ECH with cells arrested in G_2/M. Each experiment was performed in duplicate. For control assays with unsynchronized cells, 1 mL of 80-85% confluent control 6C2 chicken erythro-progenitor cells were transferred to each compartment of a six-well plate and 4 mL of fresh 6C2 growth media was added to each well (1:5 split, 5 mL final volume). Cells were incubated at 37 °C and 5% CO_2 for approximately 24 hours to allow for entry into the logarithmic growth phase. As previously stated, cells arrested in mitosis were transferred in 5 mL aliquots to five of the six wells of a six well plate after treatment with nocodazole. A 6 mL aliquot was transferred to the control well; 1 mL was removed for cell cycle analysis before the treatment assay. The procedure for synchronized cells differed from that for control cells; making 1:5 dilutions of cells arrested in G_2/M would result in 1) a period of lag phase growth during which treatment is inappropriate, 2) low concentration of cells, and 3) necessary release from mitosis in order to increase the cell concentration to that required for the flow cytometry-based cytotoxicity study.

Stock dilutions (1.0 M and 10.0 M) with 6C2 culture media were made for both DEB and ECH; each solution was made immediately preceding treatment of the cells to ensure optimal potency of the compounds. Each cytotoxicity assay tested the viability of cells under

0 mM, 2.5 mM, 10 mM, 25 mM, 100 mM, and 250 mM cross-linker for 30, 60, 120, and 180 minute treatment periods. The varying amounts of alkylating agent were added to each well to give the assigned final concentration; thorough mixing via gentle pipetting helped to diffuse the agent throughout each well. (Mixing was particularly important for ECH cytotoxicity assays as ECH formed insoluble products in the aqueous cell suspension).

At the termination of each incubation period 1 mL of cellular suspension was removed from each of the six wells and transferred to a 1.5 mL microcentrifuge tube. Samples were centrifuged at 250 x *g* for 5 minutes, after which the supernatant was removed and discarded. Visible pellets were suspended in 1 mL of 1X PBS and centrifuged as above. The supernatant was removed and discarded, and 1 mL of fresh 1X PBS added. Each suspension was transferred to a labeled flow cytometry tube. 10 µL of 50 ng/mL propidium iodide stain in 1X PBS was added to each tube. Tubes were covered with aluminum foil to protect the cellular suspension from light and incubated at room temperature for approximately 10-15 minutes.

Flow Cytometry for Cell Viability. Propidium iodide is a DNA-specific fluorescent stain; however, unlike Vybrant® DyeCycle Green™ stain, propidium iodide cannot penetrate the plasma membranes of living cells. During flow cytometric data collection, PI emission indicates cell death: apoptotic and necrotic events facilitate degradation of cellular membranes, drastically increasing permeability and allowing PI to enter the dead cell and bind to nuclear DNA. Cells that do not emit fluorescence are considered viable. Flow cytometry is a useful technique for assessing cell viability, particularly since apoptotic cells cannot be quantified by the traditional trypan blue dye exclusion test (data not shown).

Flow cytometry data was collected with BD Biosciences CellQuest™ software. FACSCalibur fluorescence detectors were set at 328 V (FL1), 605 V (FL2), and 525 V (FL3)

while the scattering detector was assigned 210 V (SSC). The mode of the FL1 detector was set to logarithmic.

Analytical dot plots were constructed for each sample of the cytotoxicity trial. A quadrant was applied to the 0 mM cross-linker, 30 minutes control sample; the lower right quadrant was fitted to the population of viable cells. The control quadrant was transposed onto all other samples to monitor shifts in the position of the population and uphold the consistency of data. Quadrant statistics listed the total number of events per quadrant.

Analysis of Data and Construction of LD_{50} Plots. Data were collected from the quadrant statistics table of each dot plot. Events occurring in the lower right quadrant (LR) were considered viable, while events in the two upper quadrants (UL + UR) represented dead cells. Events occurring in the lower left quadrant (LL) were deducted from the total number of events; such data points were determined to be inert debris existing in the culture media. The fraction of viable cells was calculated by dividing the number of events occurring in the lower right quadrant (LR) by the adjusted total events (10,000-LL).

Given that the discrete outcomes of cytotoxicity assays are binomial in nature (e.g. viable or not viable), linear and nonlinear regression models are inappropriate for analysis of data. Instead, logistic regression or probit analysis are commonly used in cytotoxicity and dose response experiments[41]. The two functions are "almost indistinguishable", but logit transformation has become increasingly popular in bioassay analysis because of its relatively simple formula[42]. In the logistic regression function,

$$P(Z) = \frac{expZ}{1 + expZ}.$$

the proportion P is the probability of the binary outcome (viable or not viable) and Z is equal to the function $\alpha + \beta X$, where α determines the location of the curve on x-axis, β

is the slope, and X represents the continuous exposure variable[42]. For the purposes of the cytotoxicity experiments, P was defined as the proportion of viable cells. Logit transformation uses the inverse of the logistic regression function to convert proportional data limited to values between 0 and 1 to an unlimited scale[42,43]:

$$logit(P) = log\frac{P}{1-P} = Z,$$

Logit transformation can makes use of $\log_{10}$ or the natural log, $\log_e$. Using Microsoft Excel, proportions of viable cells were converted to logits with the natural log function. Conveniently, the logit for P=0.50 is 0; logits for proportions greater than 0.50 are positive while logits for proportions less than 0.50 are negative. Logits for proportions 0 and 1 are infinite and cannot be calculated[43]. (This led to the exclusion of a few data points within the 180 minute incubation category, where the viable fraction had been severely diminished to zero).

Two LD_{50} plots were constructed for each of the four cytotoxicity experiments: logit versus the concentration of cross-linking agent, and logit versus the $\log_{10}$ of the concentration of cross-linking agent. Linear trendlines for 30 minutes, 60 minutes, 120 minutes, and 180 minutes were fitted to the corresponding data points by the method of least squares. LD_{50} values were calculated for each incubation period from trendline equations. Equations were chosen based on the R^2 value that represents the goodness of fit for the trendline. Additionally, smooth-line LD_{50} scatter plots for average viable fraction versus concentration of cross-linking agent were created in order to visualize the location of each incubation period dose-response curve. These plots were helpful in assessing the accuracy of the LD_{50} calculations.

Results

Synchronization of Cells. Enrichment of the percentage of 6C2 erythro-progenitor cells in G_2/M by treatment with nocodazole was largely successful, both in terms of actual synchronization and cell viability post-treatment. Preliminary experiments revealed that nocodazole successfully arrested a large percentage of cells in G_2/M with little loss of cellular integrity (Table 1). Attempts at arresting cells in G_0/G_1 with L-mimosine were mostly unsuccessful due to the prevalence of cell death after chemical treatment (data not shown). Additionally, nocodazole provided a means of synchronizing cells with low cell mortality and the option of reversible arrest, though the latter was not utilized in the current study.

Synchronization of cells for use in the duplicate DEB cytotoxicity experiment with 6C2 cells enriched in G_2/M stages (Table 1) and the ECH cytotoxicity experiment (Table 2) was relatively successful. Histograms comparing the distribution of cells in G_0/G_1 and G_2/M of untreated cells with synchronized cells illustrate a pronounced shift from G_0/G_1 to G_2/M in the second DEB assay (Figure 4). Histograms corresponding to ECH assays show slight enrichments in G_2/M but still maintain a strong G_0/G_1 peak in comparison with the second DEB assay (Figure 5).

Table 1. Histogram statistics for duplicate DEB cytotoxicity experiments with 6C2 erythro-progenitor cells enriched in G_2/M stages of the cell cycle. Table lists the percentage of cells in G_0/G_1 stages and G_2/M stages in each histogram.

	DEB G_2/M Assay I			DEB G_2/M Assay II		
Treatment	**Histogram**	**G_0/G_1 (%)**	**G_2/M (%)**	**Histogram**	**G_0/G_1 (%)**	**G_2/M (%)**
Control	A	58.3	31.6	C	52.8	37.6
Nocodazole	B	49.5	40.7	D	15.4	72.6

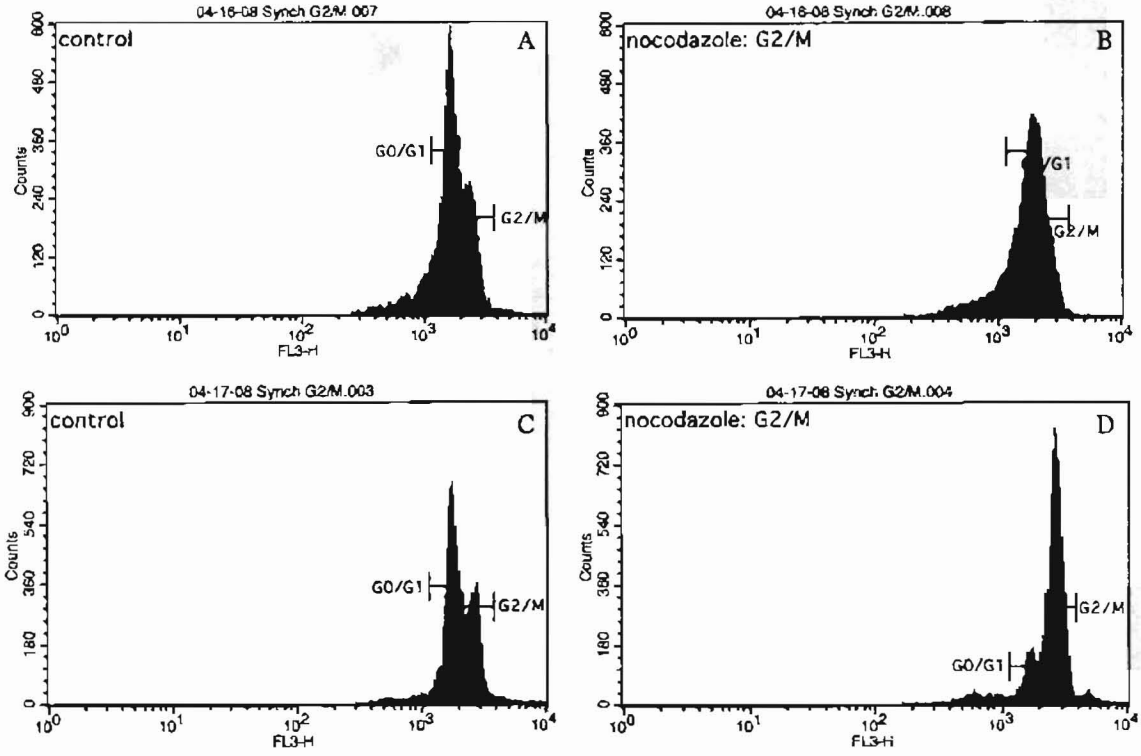

Figure 4. Histograms illustrate the relative distribution of cells throughout the stages of the cell cycle for unsynchronized control cells and cells arrested in G_2/M stages with nocodazole: DEB cytotoxicity experiments. Note the highly successful enrichment of cells in G_2/M stages by comparing histograms C and D.

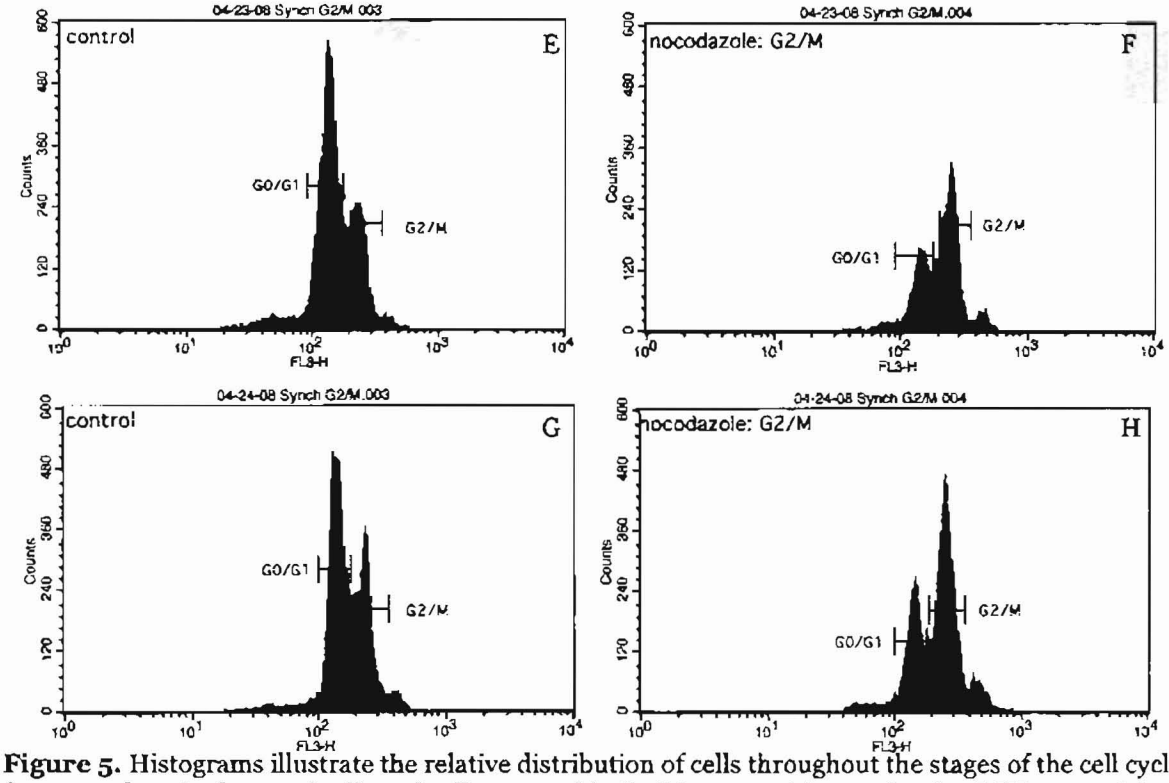

Figure 5. Histograms illustrate the relative distribution of cells throughout the stages of the cell cycle for unsynchronized control cells and cells arrested in G_2/M stages with nocodazole: ECH cytotoxicity experiments. The two synchronizations were slightly less successful in comparison to arrest in G2/M stages for the second DEB G_2/M cytotoxicity assay.

The first population of 6C2 cells treated with nocodazole for the synchronized DEB assay appeared to be mostly successful; however, analysis via gated statistics reveal that only approximately 41% of cells within the treated population were arrested in G_2/M (Table 1). 50% of cells remained in either G_0 or G_1. Increasing the distance between G_0/G_1, S, and G_2/M populations on the histogram may help with the accuracy of gate placement; the G_0/G_1 gate most likely contains a large portion of the S population. For the purposes of examining cytotoxicity in relation the presence nuclear envelope, we can assume cells in G_0, G_1 and S to be theoretically equivalent (nuclear envelope present).

Nocodazole-induced arrest of cells in G_2/M was highly successful for the population of cells used in the second DEB G_2/M assay: 72.6% of cells were arrested in G_2/M while 15.4% of cells remained in G_0/G_1 (Table 1). Given that the concentration of the cell suspension was roughly 1.0×10^6 cell/mL and each well contained 5 mL, we can calculate that approximately 5.0×10^6 cells were present in each well. Hence, 72.6% of cells translated to approximately 3.6×10^6 cells in G_2/M, and 15.4% of cells equates to about 7.7×10^5 cells in G_0/G_1. Hence, in the second DEB G_2/M assay approximately 2,860,000 *more* cells were arrested in G_2/M stages than in G_0/G_1 stages.

Table 2. Histogram statistics for duplicate ECH cytotoxicity experiments with 6C2 erythro-progenitor cells enriched in G_2/M stages of the cell cycle. Table lists the percentage of cells in G_0/G_1 stages and G_2/M stages in each histogram.

	ECH G_2/M Assay I			ECH G_2/M Assay II		
Treatment	**Histogram**	**G_0/G_1 (%)**	**G_2/M (%)**	**Histogram**	**G_0/G_1 (%)**	**G_2/M (%)**
Control	E	60.6	24.7	G	57.0	37.8
Nocodazole	F	30.2	54.2	H	30.0	58.8

Though the synchronization of cells in the G_2/M stages of the cell cycle was somewhat less pronounced within the cell populations designated for treatment with ECH, overall enrichment of cells in G_2/M was successful in both assays. Data from histograms E and F (Figure 5) indicated a 31% decrease in the G_0/G_1 population accompanied by a 30% increase in the proportion of cells arrested in G_2/M (Table 2). Reduction of the number of cells in G_0/G_1 was visually apparent between the control and nocodazole-treated histograms from the first synchronized cell ECH assay (Figure 5). 6C2 cells synchronized for use in the second assay displayed similar results. The number of cells in G_0/G_1 decreased by approximately 27%, and the G_2/M cell population grew by 21% (Table 2). Again, results were accurately represented by shifts in G_0/G_1 and G_2/M peak heights for histograms G and H (Figure 5).

While complete synchronization of cells within the G_2/M stages of the cell cycle is desirable for analysis of cell-cycle dependent cytotoxicity, simple enrichment of cells in G_2/M stages was useful to the study. The goal of synchronization was to produce a population of cells in which there existed a shift toward G_2/M stages and nuclear envelope degradation. Movement away from the control distribution and toward enrichment of G_2/M stages serves the purpose of creating a population of cells with a modified distribution of cells favoring the G_2/M stages of the cell cycle.

Cytotoxicity of DEB and ECH in 6C2 erythro-progenitor cells. To assess the relative cytotoxicity of DEB and ECH *in vivo*, viability was reported as a measure of the LD_{50}, the concentration of agent at which 50% of cells are alive. Lower LD_{50} concentrations indicate increased cytotoxicity: smaller concentrations of the agent are required to obtain cytotoxic effects. Data concerning the numbers of viable and dead cells were collected in duplicate for control DEB-treated cells and control ECH-treated cells separately via flow cytometry with propidium iodide. The viable fractions of cells were calculated from the raw data for each concentration of agent at the designated exposure time. The proportion of viable cells was

transformed with logistic regression to fit a normal distribution curve. The logit, which is equal to the natural log of the viable fraction divided by the proportion of dead cells, was plotted against the concentration of agent or the log of the concentration of agent in Microsoft Excel (Figures 6 and 7). These plots provided a linear relationship between the viability (logit) and the concentration of DEB or ECH. Linear trendlines were fit to data from each incubation period by the method of least squares. Linear trendline equations in the y= mx + b form and corresponding R^2 values were recorded from both plots. Equations for use in the calculation of LD_{50} concentrations were selected on the basis of "goodness of fit" as indicated by R^2 values; the equation with the R^2 value closest to 1.0 was consistently used to calculate LD_{50} concentrations (Tables 3 and 4). Smooth-line scatter plots of the average viable fraction versus the concentration of agent were also created in Excel to visualize the shape of the sigmoidal dose-response curve for each of the cytotoxicity experiments (Figures 6 and 7).

DEB LD_{50} concentrations for 30 minute, 60 minute, 120 minute, and 180 minute incubation periods were calculated to be 168 mM, 110 mM, 10.2 mM, and 4.54 mM, respectively (Table 5). As indicated, 30 minute and 60 minute LD_{50} concentrations were derived from the logit v. [DEB] (mM) scatter plot whereas the LD_{50} concentrations for the 120 minute and 180 minute data sets were calculate from the equations given by the logit vs. log[DEB] scatter plot (Table 3). Variations in linear fit between the data sets may be attributed to the shallow sigmoidal curve of 30 minute and 60 minute data in comparison to the very steep dose response curve for 120 minute and 180 minute data (Figure 6).

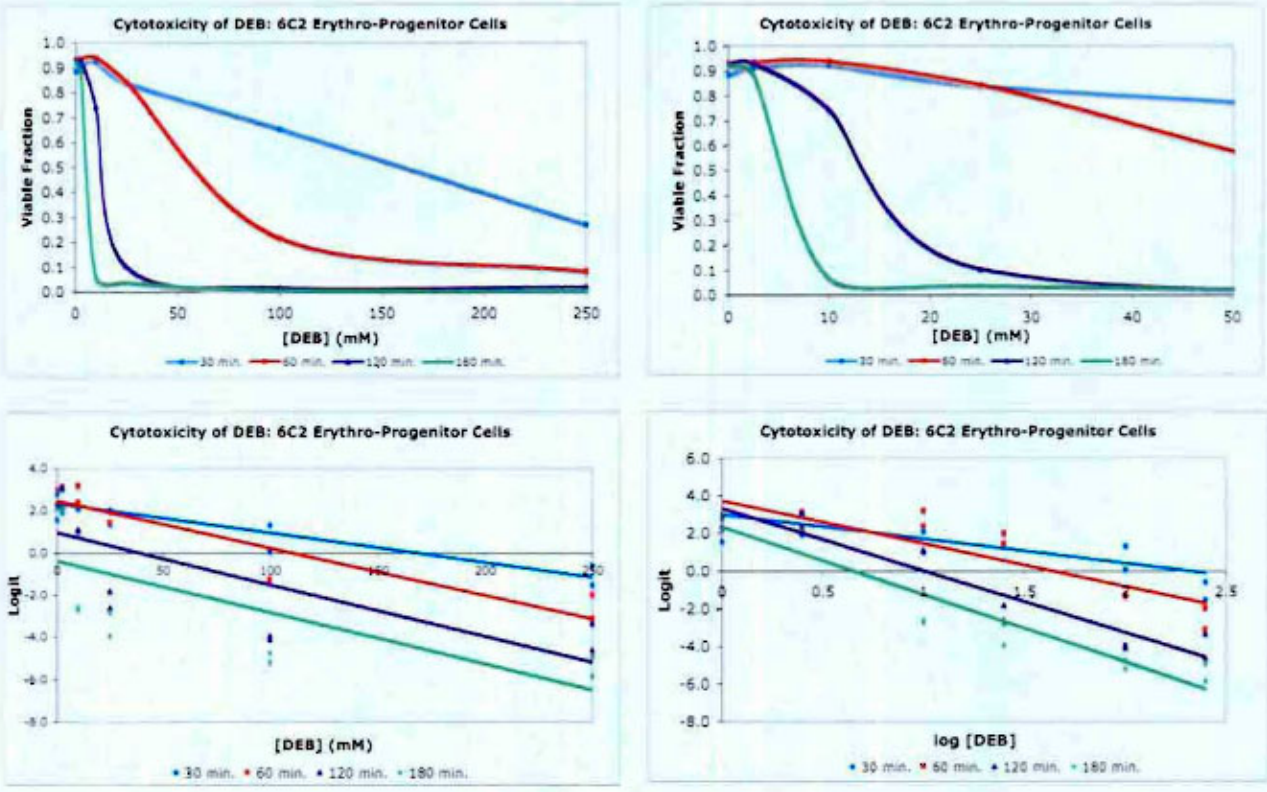

Figure 6. LD_{50} plots for the cytotoxicity of DEB in unsynchronized control 6C2 erythro-progenitor cells. Smooth line scatter plots of the average viable fraction versus the concentration of DEB were helpful in visualizing each sigmoidal dose response (upper left and upper right).

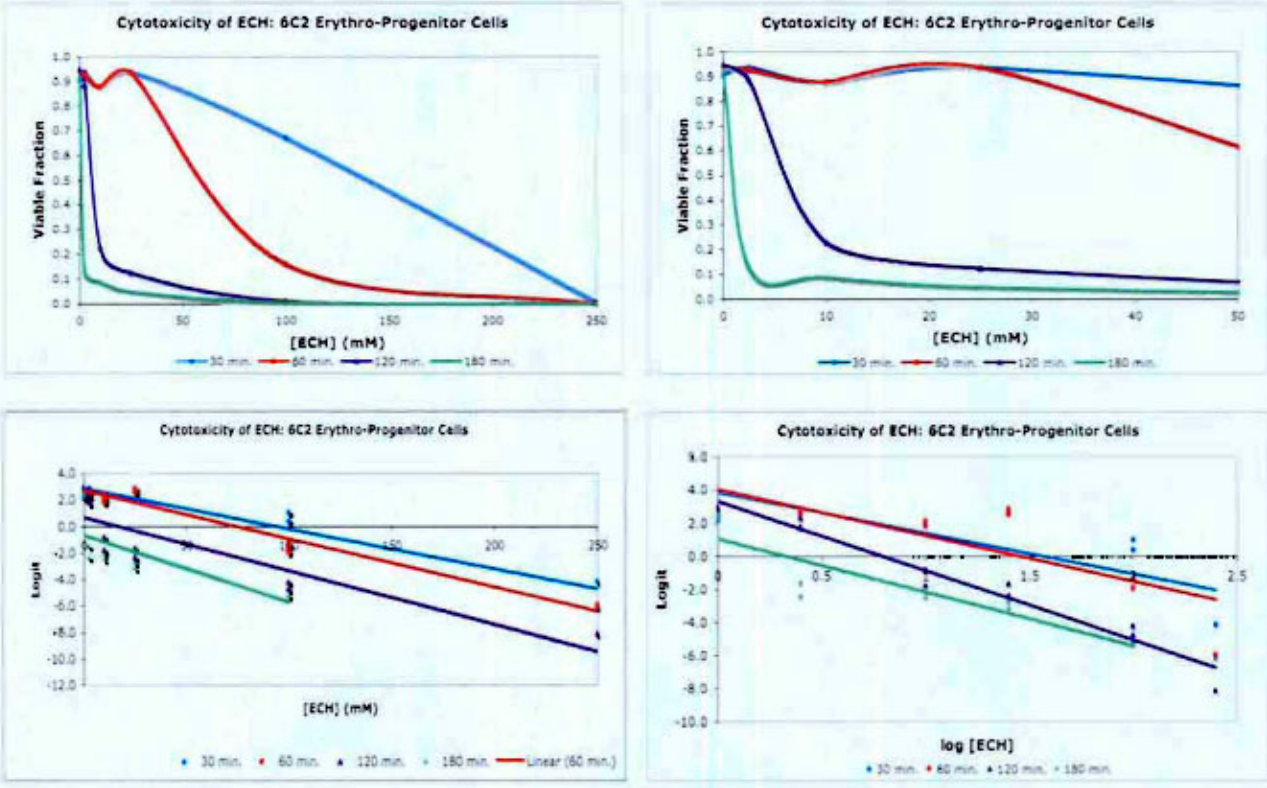

Figure 7. LD_{50} plots for the cytotoxicity of ECH in unsynchronized control 6C2 erythro-progenitor cells. Smooth line scatter plots illustrated the sigmoidal shape of each dose response curve (upper left and upper right).Logistic transformation did not allow for use of 180 minutes, 250 mM ECH data: the logit of 0 is infinite.

Table 3. Equation components and R^2 values for linear trendlines of the logit vs. [DEB] (mM) and logit vs. log[DEB] scatter plots for the unsynchronized control DEB cytotoxicity experiment. Equations highlighted in blue were used to calculate LD_{50} concentrations.

Cytotoxicity of DEB: 6C2 Erythro-Progenitor Cells				Cytotoxicity of DEB: 6C2 Erythro-Progenitor Cells			
Logit v. [DEB] (mM)	Slope	Y-Intercept	R^2	Logit v. log[DEB]	Slope	Y-Intercept	R^2
30 min.	-0.0140	2.35	0.819	**30 min.**	-1.29	3.00	0.615
60 min.	-0.0223	2.45	0.859	**60 min.**	-2.27	3.73	0.782
120 min.	-0.0246	0.956	0.579	**120 min.**	-3.29	3.31	0.908
180 min.	-0.0245	-0.361	0.485	**180 min.**	-3.58	2.35	0.912

Table 4. Equation components and R^2 values for linear trendlines of the logit vs. [ECH] (mM) and logit vs. log[ECH] scatter plots for the unsynchronized control ECH cytotoxicity experiment. Equations highlighted in yellow were used to calculate LD_{50} concentrations.

Cytotoxicity of ECH: 6C2 Erythro-Progenitor Cells				Cytotoxicity of ECH: 6C2 Erythro-Progenitor Cells			
Logit v. [ECH] (mM)	Slope	Y-Intercept	R^2	Logit v. log[ECH]	Slope	Y- Intercept	R^2
30 min.	-0.0303	2.88	0.935	**30 min**	-2.46	3.87	0.541
60 min.	-0.0366	2.73	0.959	**60 min.**	-2.78	4.02	0.651
120 min.	-0.0404	0.696	0.762	**120 min.**	-4.19	3.33	0.959
180 min.	-0.0505	-0.642	0.560	**180 min.**	-3.23	1.07	0.827

Like the incubation period data sets in the control DEB cytotoxicity study, 30 minute and 60 minute data sets exhibited a shallow sigmoidal dose reponse curve and exhibited greater R^2 values by the plot of logit v. [ECH] (mM), whereas 120 minute and 180 minute data displayed very steep dose reponse curves and were better suited to the logit v. log[ECH] plot (Figure 7). Equations for 30 minute, 60 minute, and 120 minute linear trendlines had optimal R^2 values ranging from 0.93 to approximately 0.96. The trendline used for analysis of 180 minute incubation period data had an R^2 value of 0.827 (Table 4). The decreased accuracy of fit may be due to the required omission of 180 minute, 250 mM ECH data points. LD_{50} concentrations of ECH for the 30 minute, 60 minute, 120 minute, and 180 minute incubation periods of the control ECH cytotoxicity study were 94.9 mM, 74.6 mM, 6.24 mM, and 2.14 mM, respectively (Table 5).

Table 5. LD_{50} concentrations for DEB and ECH cytotoxicity experiments with unsynchronized control 6C2 erythro-progenitor cells.

	Control, Unsynchronized 6C2 Cells	
Length of Treatment	**DEB LD_{50} (mM)**	**ECH LD_{50} (mM)**
30 min.	168	94.9
60 min.	110	74.6
120 min.	10.2	6.24
180 min.	4.54	2.14

Cytotoxicity of DEB and ECH in 6C2 erythro-progenitor cells enriched in G_2/M stages of the cell cycle. Cytotoxicity studies monitoring cell viability as a function of the concentration of agent were performed for 6C2 erythro-progenitor cells enriched in G_2/M stages of the cell cycle. The objective of the experiments was to determine the role of the nuclear envelope in inhibition of the cytotoxic action of DEB and ECH. After successful enrichment of cells in the G_2/M stages of the cell cycle by treatment with nocodazole, 6C2 cells were treated with varying concentrations of DEB and ECH (individually) for 30 minute, 60 minute, 120 minute, and 180 minute incubation periods. Post-treatment cell viability was assessed via flow cytometry. Following the experimental procedures and analytical methods used in the cytotoxicity experiments with unsynchronized control 6c2 cells allowed us to compare the LD_{50} cytotoxicity results for DEB and ECH between unsynchronized and synchronized cell populations. Additionally, inferences were made about the cytotoxicity of DEB in comparison to ECH in terms of unsynchronized and G_2/M enriched cell experiments.

LD_{50} concentrations for the 30 minute, 60 minute, 120 minute, and 180 minute incubation periods of the DEB cytotoxicity experiment with 6C2 cells enriched in G_2/M stages were 68.9 mM, 81.9 mM, 19.6 mM, and 8.29 mM, respectively (Table 6). The smooth line scatter plot for the average viable fraction versus the concentration of agent illustrated that each of the four dose response curves were relatively similar in shape and slope (Figure 8). Slopes and R^2 values were comparable between the two logistic regression plots for all treatments (Table 7).

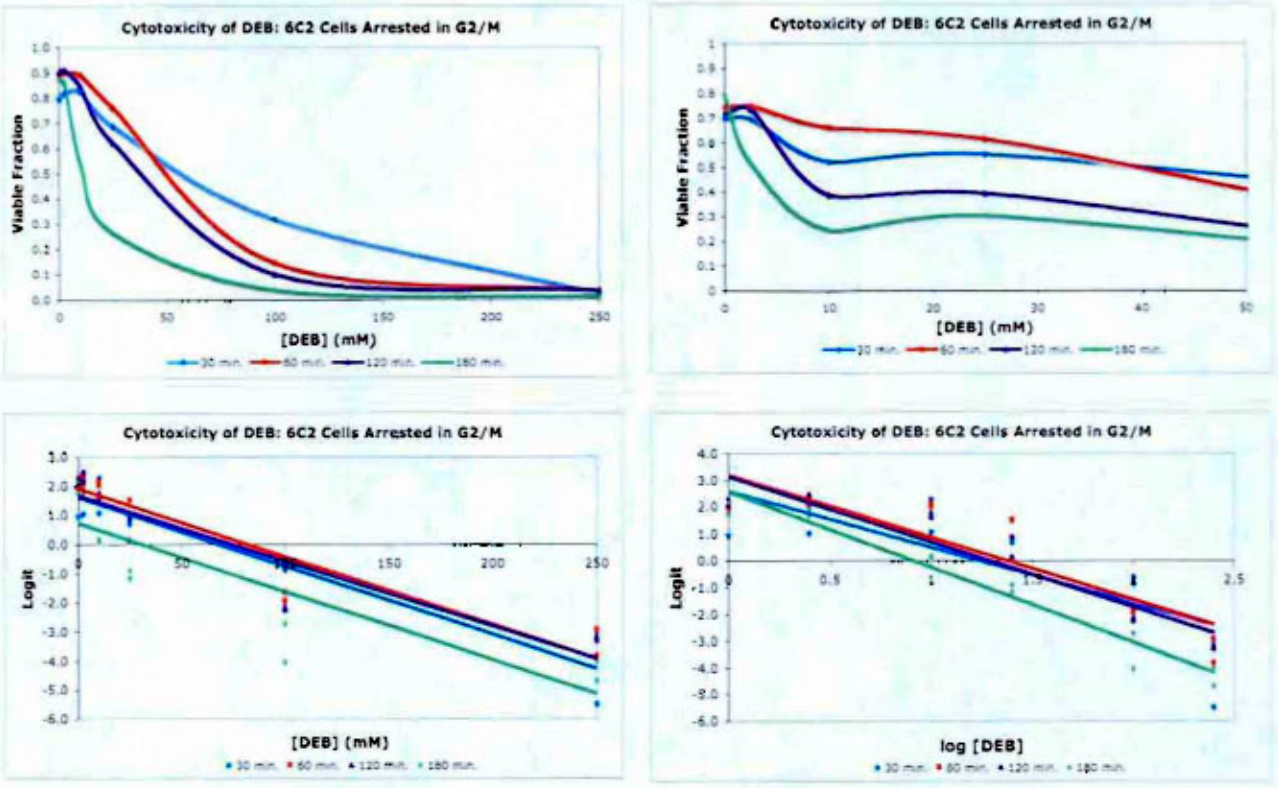

Figure 8. LD_{50} plots for the cytotoxicity of DEB in 6C2 erythro-progenitor cells enriched in G_2/M stages of the cell cycle. Smooth line scatter plots illustrated the sigmoidal shape of each dose response curve (upper left and upper right). Unlike the control DEB cytotoxicity experiment, the dose response curves of 30 minute and 60 minute data sets were similar to that of 120 minute and 180 minute data (upper left).

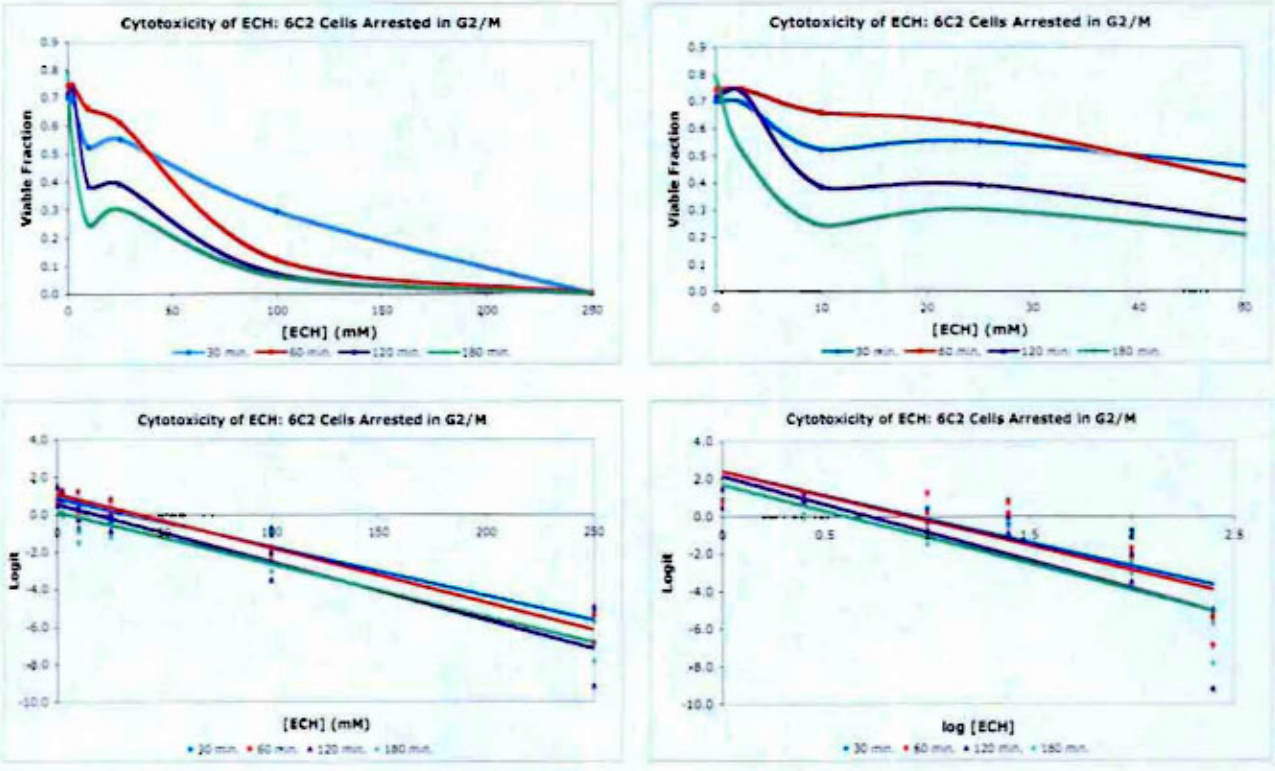

Figure 9. LC_{50} plots for the cytotoxicity of ECH in 6C2 erythro-progenitor cells enriched in G_2/M stages of the cell cycle. Smooth line scatter plots illustrate the sigmoidal shape of each dose response curve (upper left and upper right). Interestingly, the 30 minute and 60 minute dose response curves intersect at a concentration of approximately 40 mM ECH (upper right and upper left).

Viability data from the ECH cytotoxicity experiment with 6C2 cells enriched in G_2/M stages is unique in that the relationship between viability and concentration of ECH was best characterized by the logit v. [ECH] (mM) plot for all four incubation period data sets (Table 8). Dose response curves created for this experiment are notably shallower than those produced in the other three experiments, but also resemble dose response curves of the cytotoxicity of DEB synchronization in G_2/M experiment (Figure 8, Figure 9). Additionally, the fit of the linear trendlines to data was exceptionally strong, with R^2 values ranging from approximately 0.87 to 0.97 (Table 8). The LD_{50} concentrations for 30 minutes, 60 minute, 120 minutes, and 180 minutes incubation periods within the cytotoxicity of ECH synchronization experiment were 34.0 mM, 37.6 mM, 17.9 mM, and 4.89 mM, respectively (Table 6).

Table 6. LD_{50} concentrations for DEB and ECH cytotoxicity experiments with 6C2 erythro-progenitor cells enriched in G_2/M stages of the cell cycle.

	Synchronized 6C2 Cells (G_2/M)	
Length of Treatment	**DEB LD_{50} (mM)**	**ECH LD_{50} (mM)**
30 min.	68.9	34.0
60 min.	81.9	37.6
120 min.	19.6	17.9
180 min.	8.29	4.89

Table 7. Equation components and R^2 values for linear trendlines of the logit vs. [DEB] (mM) and logit vs. log[DEB] scatter plots for the DEB cytotoxicity experiment with 6C2 cells enriched in G_2/M stages of the cell cycle. Equations highlighted in blue were used to calculate LD_{50} concentrations.

Cytotoxicity of DEB: 6C2 Cells Arrested in G_2/M				Cytotoxicity of DEB: 6C2 Cells Arrested in G_2/M			
Logit v. [ECH] (mM)	Slope	Y-Intercept	R^2	Logit v. log [DEB]	Slope	Y- Intercept	R^2
30 min.	-0.0234	1.61	0.906	**30 min**	-2.09	2.61	0.638
60 min.	-0.0233	1.91	0.901	**60 min.**	-2.34	3.21	0.800
120 min.	-0.0223	1.67	0.842	**120 min.**	-2.44	3.15	0.887
180 min.	-0.0233	0.721	0.753	**180 min.**	-2.81	2.58	0.957

Table 8. Equation components and R^2 values for linear trendlines of the logit vs. [ECH] (mM) and logit vs. log[ECH] scatter plots for the ECH cytotoxicity experiment with 6C2 cells enriched in G_2/M stages of the cell cycle. Equations highlighted in yellow were used to calculate LD_{50} concentrations.

Cytotoxicity of ECH: 6C2 Cells Arrested in G_2/M				Cytotoxicity of ECH: 6C2 Cells Arrested in G_2/M			
Logit v. [ECH]	Slope	Y-Intercept	R^2	Logit v. log[ECH]	Slope	Y- Intercept	R^2
30 min.	-0.0261	0.887	0.922	**30 min**	-2.51	2.38	0.590
60 min.	-0.0290	1.09	0.972	**60 min.**	-2.63	2.37	0.700
120 min.	-0.0309	0.552	0.874	**120 min.**	-2.99	2.14	0.718
180 min.	-0.0278	0.136	0.901	**180 min.**	-2.80	1.70	0.803

Discussion

Comparison of control DEB and ECH cytotoxicity studies indicates that ECH is slightly more cytotoxic to 6C2 erythro-progenitor cells than DEB at brief incubation periods, but is comparable in cytotoxicity for longer exposure times (Table 5). Evaluation of DEB and ECH cytotoxicity experiments with 6C2 cells arrested in G2/M stages revealed that the overall cytotoxicity of both bifunctional alkylators was greater in synchronized 6C2 cell populations enriched in G_2/M stages of the cell cycle (Table 6). Again, ECH is more cytotoxic than DEB at incubation times less than 60 minutes but has similar cytotoxicity for treatment times over one hour. ECH may have displayed greater cytotoxicity due to its insolubility in aqueous cell suspensions. Some of the ECH added to the 6C2 cell suspension precipitated out of solution and most likely killed cells located on the bottom of the wells.

Results from the cytotoxicity experiments support the treatment of 6C2 cells with 250 mM of DEB, ECH, and EBH in previously conducted QPCR studies. 6C2 cells were incubated with varying concentrations (0.025 mM—250 mM) of bifunctional alkylating agent for varying times (15 min.—180 min.). QPCR analysis revealed that at a constant incubation time of 1 hour there was little loss of PCR products (result of DNA damage) for concentrations less than the 250 mM[35]. Thus, subsequent cross-linking experiments used 250 mM of agent.

After submitting the manuscript titled, "Quantitative PCR analysis of diepoxybutane and epihalohydrin damage to nuclear versus mitochondrial DNA[35]" for publication, we received referee reports that stated that DEB induces extreme toxicity at a concentration of 10 μM. The reviewers requested that we provide dose-dependent survival curves in the chicken 6C2 erythro-progenitor cells exposed to 2.5 mM to 250 mM of agent for various time intervals, and explore the mechanism of cell death triggered by the agents.

These experiments show that at 30 minutes of treatment, nearly half of the 6C2 cell population survived doses of 168 mM DEB and 95 mM ECH (Table 5). Our reviewers deemed

such "mega-doses" as inappropriate; however, results indicate that 6C2 cells are able to withstand exposure to large doses of DEB or ECH for short periods of time. We chose brief incubation periods to maintain the synchrony of arrested cells; incubation of 6C2 cells with low doses of DEB or ECH for extended periods of time may disrupt synchrony and population size. Furthermore, current work in the Millard Biochemistry Research Lab demonstrates that incubation conditions of 20 μM agent over 4 hours doesn't induce significant cytopathologies, whereas 1 mM agent over 4 hours is sufficient for passage into late apoptosis in our 6C2 cell line (Annexin V/propidium iodide stain)[44]. Future work will investigate the concentrations of DEB and ECH required to induce apoptosis at 15 minute, 30 minute, and 1 hour incubation times.

Both DEB and ECH experiments indicated that these two bifunctional alkylators are more cytotoxic during G_2/M than during the other stages of the cell cycle, specifically the G_0/G_1 interface and G_1 population. These results may indicate the role of the nuclear envelope (and other cellular membranes, such as the mitochondrial inner membrane) in excluding small, relatively polar molecules. Conversely, initial mortality by chemical synchronization agents may have increased the cytotoxicity of DEB and ECH within the 30 minute and 60 minute treatment periods; this possibility necessitates exploration into the effect of the starting viability on logistic regression models.

Interestingly, an increase in cytotoxicity during G_2/M stages was noted for 30 minute and 60 minute incubation times, but little difference was observed in LD_{50} concentrations for 120 minute and 180 minute data sets. Examination of the smooth line scatter plots shows that the dose response curves for 120 minutes and 180 minutes are relatively steep for both control and synchronized cells. However, the shape of the 30 minute and 60 minute curves was shallow within the control experiments and became increasingly sigmoidal with arrest in G_2/M stages.

This phenomenon may be due to logistic transformation of sigmoidal data to a linear relationship. Low initial viability translates into a more negative logit and smaller Y-intercept. Given that the viable fraction is limited to values of 0 to 1, the high cytotoxicity (low LD_{50} value and lower viable fractions for smaller concentrations) of a compound will limit the slope of the line. In comparing the slopes of the cytotoxicity of ECH control study (Table 4) and the cytotoxicity of ECH synchronization experiment (Table 8) we find that the slopes of the equations for data in the synchronization experiment are smaller, resulting in a shallow trendline. Leveling of the slope may actually increase the calculated viable fraction for a specific concentration, making it seem that the cytotoxicity of the compound decreases with time.

While the initial results of these cytotoxicity studies are promising, other considerations call for a larger sample size (triplicate or quadruplicate trials for each assay) and the exploration of additional statistical methods of determining an LD_{50} from a sigmoidal dose response curve. Logistic regression requires that raw data undergo transformation to abstract values in order to fit the data to a linear model. Transformation increases the complexity of calculating standard deviations and standard errors of individual data points, resulting in a statistical nightmare for all those who attempt it without working knowledge of computer-based stats packages. Using a curve-fitting program would be beneficial in that it allows for the calculation of standard deviations and the ability to more confidently define the relationship between variables. One possibility is the least squares curve fitting solver tool in Excel that fits sigmoidal curves to data on a logarithmic scale. The program uses a hyperbolic equation: $1/(1 + (x/a)^b)$, where x is the proportion of interest, and a is solved as the LD_{50} concentration[45].

Additionally, thorough exploration of the effects of the cell cycle on the cytotoxicity of DEB and ECH requires alternative methods for synchronization of cells in G_0/G_1 and S in

addition to G_2/M stages. Future goals include the complete comparison of DEB and ECH cytotoxicity for each stage of the cell cycle.

Conclusion

Our results suggest that ECH is more cytotoxic than DEB in both unsynchronized control 6C2 erythro-progenitor cells and synchronized 6C2 erythro-progenitor cells enriched in G_2/M stages of the cell cycle. Treatment with either bifunctional alkylating agent induced greater cytotoxicity in 6C2 cells enriched in G_2/M stages than in unsynchronized control 6C2 cells. Furthermore, data supports the use of 250 mM DEB and ECH in the previous QPCR study as 6C2 cells can withstand "mega-doses" of each agent. Based on previous studies, we believe that the cytotoxic effects of DEB and ECH result from DNA damage from the formation of DNA adducts and covalent DNA interstrand cross-links[6,12,13,14,15,21]. Greater cytotoxicity of both agents in 6C2 cells enriched in G_2/M stages of the cell cycle suggests that the presence of the nuclear envelope—or any plasma membrane—may inhibit the reactivity of DEB and ECH. Further work with a greater number of replicate assays and dose-response curve fitting models is required to determine the statistical significance of our results.

References

[1] Twombly, R. (2005) Cancer Surpasses Heart Disease as Leading Cause of Death for All But the Elderly. *J. Natl. Cancer Inst.* 97, 330-331.

[2] American Cancer Society. *Cancer Facts & Figures.* Atlanta: American Cancer Society: 2008.

[3] Kohn, K. W. (1996) Beyond DNA Cross-Linking: History and Prospects of DNA-targeted Cancer Treatment—Fifteenth Bruce F. Cain Memorial Award Lecture. *Cancer Research* 56, 5533-5546.

[4] Millard, J. T., and White, M. M. (1993) Diepoxybutane Cross-Links DNA at 5'-GNC Sequences. *Biochemistry* 32, 2120-2124.

[5] Millard, J. T., and Wilkes, E. E. (2001) Diepoxybutane and Diepoxyoctane Interstrand Cross-Linking of the 5S DNA Nucleosomal Core Particle. *Biochemistry* 40, 10677-10685.

[6] Gasparutto, D., Michel, T., Ramirez-Fuentes, T., Saint-Pierre, C., and Cadet, J. (2005) Epoxide adducts at the guanine residue within single-stranded DNA chains: Reacitivity and stability studies. *Nucleosides, Nucleotides, and Nucleic Acids* 24, 525-552.

[7] Helleday, T., Peterman, E., Lundin, C., Hodgson, B., and Sharma, R. A. (2008) DNA repair pathways as targets for cancer therapy. *Nature Reviews Cancer* 8,193-204.

[8] Kligerman, A. D., and Hu, Y. (2007) Some insights into the mode of action of butadiene by examining the genotoxicity of its metabolites. *Chem.-Biol. Interact. 166*, 132-139.

[9] Park, S., Anderson, C., Loeber, R., Seetharaman, M., Jones, R., and Tretyakova, N. (2005) Interstrand and Intrastrand DNA—DNA Cross-Linking by 1,2,3,4-Diepoxybutane: Role of Stereochemistry. *J. Am. Chem. Soc. 127,* 14355-14356.

[10] Occupational Safety and Health Administration. (05 Jul. 1989). Section 6—VI. Health Effects Discussion and Determination of Final PEL. Retrieved 20 March 2008, from <http://www.osha.gov/pls/oshaweb/owadisp.show_document?p_table= PREAMBLES&p_id=770>

[11] Occupational Safety and Health Administration. (04 Nov. 1996). Occupational Exposure to 1,3-Butadiene. Retrieved 20 March 2008, from <http://www.osha.gov/pls/oshaweb/owadisp.show_document?p_table= FEDERAL_REGISTER&p_id=13585>

[12] Divine, B. J., Wendt, J. K., Hartman, C. M. (1993) Cancer mortality among workers at a butadiene production facility, in *Butadiene and Styrene: Assessment of Health Hazards* (Sorsa, M., Peltonen, K., Vainio, H., Hemminki, K., Eds.) 345-362, IARC Scientific Publications No. 127, IARC, Lyon.

[13] Divine, B. J., and Hartman, C. M. (2001) A cohort mortality study among workers at a 1,3 butadiene facility, *Chem.-Biol. Interact. 135-136*, 535-553.

[14] Delzell, E., Macaluso, M., Sathiakumar, N., and Matthews, R. (2001) Leukemia and exposure to 1,3-butadiene, styrene, and dimethyldithiocarbamate among workers in the synthetic rubber industry, *Chem.-Biol. Interact.135-136*, 515-534.

[15] IARC. (14 Apr. 1999) Volume 71: Re-Evaluation of Some Organic Chemicals, Hydrazone, and Hydrogen Peroxide. Retrieved 30 April 2008, from <http://monographs.iarc.fr/ENG/Monographs/vol71/volume71.pdf>

[16] Seyschab, H., Friedl, R., Sun, Y., Schindler, D., Hoehn, H., Hentze, S., and Schroeder-Kurth, T. (1995) Comparitive Evaluation of Diepoxybutane Sensitivity and Cell Cycle Blockage in the Diagnosis of Fanconi Anemia. *Blood 85*, 2233-2237.

[17] Centurion, S., Kuo, H-R., and Lambert, W. C. (2000) Damage-Resistant DNA Synthesis in Fanconi Anemia Cells Treated with a DNA Cross-Linking Agent. *Exp. Cell Res. 260*, 216-221.

[18] Sala-Trepat, M., Rouillard, D., Escarceller, M., Laquerbe, A., Moustacchi, E., and Papadopoulo, D. (2000) Arrest of S-Phase Progression Is Impaired in Fanconi Anemia Cells. *Exp. Cell Res. 260*, 208-215.

[19] Sawyer, G. A., Frederick, E. D., and Millard, J.T. (2004) Flanking Sequences Modulate Diepoxide and Mustard Cross-linking Efficiencies at the 5'-GNC Site. *Chem. Res. Toxicol. 17*, 1057-1063.

[20] Kolman, A., Chovanec, M., and Osterman-Golkar, S. (2002) Genotoxic effects of ethylene oxide, propylene oxide and epichlorohydrin in humans: update review (1990-2001). *Mut. Res. 512*, 173-194.

[21] Van Duuren, B. L., and Goldschmidt, B. M. (1966) Carcinogenicity of Epoxides, Lactones, and Peroxy Compound. III. Biological Activity and Chemical Reactivity. *J. Medicinal Chem. 9*, 77-79.

[22] Sund, P., and Kronberg, L. (2006) Reaction of epichlorohydrin with adenosine, 2'-deoxyadenosine and calf thymus DNA: Identification of adducts. *Bioorganic Chem. 34*, 115-130.

[23] Romano, K. P., Zahran, R. W., Newman, A. G., and Millard, J. T. (2007) DNA Interstrand Cross-Linking by Epichlorohydrin. *Chem. Res. Toxicol. 20*, 832-838.

[24] Murray, Andrew and Tim Hunt. *The Cell Cycle: An Introduction*. New York: W. H. Freeman, 1993.

[25] Hartwell, L. H., and Kastan, M. B. (1994) Cell Cycle Control and Cancer. *Science 266*, 1821-1828.

[26] Ford, H. L., and Pardee, A. B. (1999) Cancer and the Cell Cycle. *J Cell. Biochem. Supp 32/33*, 166-172.

[27] Mercer, E. W. (1998) Checking on the Cell Cycle. *J. Cell. Biochem. Supp. 30/31*, 50-54.

[28] Lenart, P., and Ellenberg, J. (2006) Monitoring the permeability of the nuclear envelope during the cell cycle. *Methods 38*, 17-24.

[29] Cavenee, W. K., and White, R. L. The Genetic Basis of Cancer: An accumulation of genetic defects can apparently cause normal cells to become cancerous and cancerous cells to become increasingly dangerous. *Scientific American*, March 1995, 72-79.

[30] Weinberg, R. A. How Cancer Arises: An explosion of research is uncovering the long-hidden molecular underpinnings of cancer—and suggesting new therapies. *Scientific American*, September 1996, 62-70.

[31] Zhou, B-B. S., and Elledge, S. J. (2000) The DNA damage response: putting checkpoints in perspective. *Nature 408*, 433-439.

[32] Mlejnek, P., and Kolman, A. (1999) Effects of three epoxides—ethylene oxide, propylene oxide, and epichlorohydrin—on cell cycle progression and cell death in human diploid fibroblasts. *Chem-Biol. Interact. 117*, 219-239.

[33] Ayala-Torres, A., Chen, Y., Svoboda, T., Rosenblatt, J., and Van Houten, B. (2000) Analysis of Gene-Specific DNA Damage and Repair Using Quantitative Polymerase Chain Reaction. *Methods 22*, 135-147.

[34] Newman, A. G. (2007) Quantitative PCR Reveals Preferential Nuclear DNA Alkylation by ECH in the Chicken Genome. Colby College Dept. of Chemistry.

[35] LaRiviere, F. J., Newman, A. G., Watts, M. L., Juskewitch, J. E., Greenwood, P. G., and Millard, J. T. (2008) Quantitative PCR analysis of diepoxybutane and epihalohydrin damage to nuclear versus mitochondrial DNA. *manuscript in preparation

[36] Backer, J. M., and Weinstein, I. B. (1980) Mitochondrial DNA is a major cellular target for a dihydrodiol-epoxide derivative of benxo[*a*]pyrene. *Science 209*, 297-299.

[37] Jackman, J. and P. M. O'Connor. (1998) Methods for Synchronizing Cells at Specific Stages of the Cell Cycle. In *Current Protocols for Cell Biology*, John Wiley & Sons, 1998.

[38] "Nocodazole." Sigma Aldrich: Products for Life Science Research 2008-2009. p. 1418.

[39] Clute, P., and Pines, J. Temporal and spatial control of cyclin B1 destruction in metaphase. *Nature Cell Biology 1*, 82-87.

[40] Molecular Probes: Invitrogen Detection Technologies. Product Information: Vybrant DyeCycle Stains. Revised 10 October 2006.

[41] Motulsky, Harvey and Arthur Christopoulos. *Fitting Models to Biological Data Using Linear and Nonlinear Regression: A Practical Guide to Curve Fitting*. New York: Oxford University Press, 2004.

[42] Cramer, J. S. Chapter 9: The origins and development of the logit model. In *Logit Models from Economics and Other Fields*. Cambridge University Press, 2003.

[43] Dytham, Calvin. *Choosing and Using Statistics: A Biologist' Guide*, 2nd Ed. Malden, MA: Blackwell Publishing, 2003.

[44] Stein, M. J. (2008) Determining the mechanism of cell death induced by diepoxybutane and epichlorohydrin. Senior Research Project, Dept. of Chemistry, Colby College. Unpublished data.

[45] Rice, K. P., Penketh, P. G., Shyam, K., and Sartorelli, A. C. (2005) Differential inhibition of cellular glutathione reductase activity by isocyanates generated from the antitumor prodrugs Cloretazine™ and BCNU. *Biochemical Pharmacology* 69, 1463-1472.